AIP | The Journal of Chemical Physics

Influence of restricted geometries on the direct energy transfer

A. Blumen, J. Klafter, and G. Zumofen

Citation: The Journal of Chemical Physics **84**, 1397 (1986); doi: 10.1063/1.450481
View online: http://dx.doi.org/10.1063/1.450481
View Table of Contents: http://scitation.aip.org/content/aip/journal/jcp/84/3?ver=pdfcov
Published by the AIP Publishing

Influence of restricted geometries on the direct energy transfer

A. Blumen[a)] and J. Klafter
Corporate Research Science Laboratories, Exxon Research and Engineering Company, Annandale, New Jersey 08801
G. Zumofen
Laboratorium für Physikalische Chemie, ETH-Zentrum, CH-8092 Zürich, Switzerland

(Received 10 October 1984; accepted 17 October 1985)

We investigate the direct energy transfer from a donor to acceptors embedded in spaces with restricted geometries. The decay of the donor is expressed in terms of a site density function $\rho_0(\mathbf{r})$ which depends on the position of the donor within the structure. For randomly distributed donors one has to average over their locations. We focus on spherical and cylindrical shapes. The geometrical restrictions manifest themselves in deviations from the known Förster direct transfer behavior.

I. INTRODUCTION

Direct energy transfer from an excited donor molecule to randomly distributed acceptor molecules in condensed media has been of considerable interest for a long time.[1–3] Following the pioneering work of Förster the direct energy transfer has been extensively studied experimentally[4,5] and theoretically[6–11] both in solids[4–6] and in liquids.[12,13]

In most cases it has been assumed that the systems under study are infinite and that the average density of molecules is constant. Theories based on these assumptions have been shown to be very successful in interpreting energy transfer in many materials.[6,12,13] There are however, physical systems where energy transfer cannot be modeled by an infinite volume with a constant average density of molecules inside it. Examples are micellar systems[14,15] zeolite structures characterized by connected cages,[16] polymer coils in solutions,[17] and porous glasses.[18,19] Common to these examples is that the molecules participating in the energy transfer process occupy sites on restricted geometries. The geometrical restrictions differ among the various systems. For micelles, one usually assumes a constant acceptor density within a finite volume.[17] In polymer systems, one faces the situation where the locations of the molecules are correlated by the polymer bonds[17] and in addition, the coils have finite extent. The spatial restriction on the donor and acceptor sites inside the pores of a porous glass has recently been modeled both by a fractal picture[19,20] and by a network of cylinders.[21]

In a previous paper[22] we proposed that energy transfer methods may be used for characterization of complex structures such as fractals. Here we extend our results to include more general cases of restricted geometries. We focus our attention on the general formulation of the decay of a donor due to the presence of acceptors and we follow the development as far as possible by analytical methods. We concentrate on several examples involving spherical and cylindrical shapes and display graphically the crossover effects which are due to spatial restrictions. Thus, these decay laws show a richer behavior than the one for regular infinite lattices.

II. THE DIRECT ENERGY TRANSFER

In the classical problem of direct energy transfer[1] one considers an excited donor molecule, at position $\mathbf{r}_0$, surrounded by acceptors which occupy some of the sites $\mathbf{r}_i$ of a given structure. The transfer rates $w(\mathbf{r})$ depend on the mutual distance $\mathbf{r}$ between each donor–acceptor pair. Neglecting back transfer, the probability of the decay of the donor due to the presence of an acceptor at $\mathbf{r}_i$ is thus

$$f(t, \mathbf{r}_i, \mathbf{r}_0) = \exp[-tw(\mathbf{r}_i - \mathbf{r}_0)] . \qquad (1)$$

One assumes the acceptors to act independently, which means that they contribute multiplicatively to the decay. Let $g(j)$ be the probability of having j acceptors at one site. The decay of the donor is given by

$$\Phi(t, \mathbf{r}_0) = \prod_{\mathbf{r}_i}{}' \left\{\sum_j g(j)\,[f(t, \mathbf{r}_i, r_0)]^j\right\}, \qquad (2)$$

where the product extends over all structure sites with the exception of $\mathbf{r}_0$. Thus, for a binomial distribution, $g(j) = (1-p)\delta_{0,j} + p\delta_{1,j}$ ($\delta_{i,j}$ being the Kronecker delta) one has

$$\Phi(t, \mathbf{r}_0) = \prod_{\mathbf{r}_i}{}' \{1 - p + p\exp[-tw(\mathbf{r}_i - \mathbf{r}_0)]\} . \qquad (3)$$

For a small acceptor concentration, $p \ll 1$, one may replace Eq. (3) by

$$\tilde{\Phi}(t, \mathbf{r}_0) = \exp\left(-p \sum_{\mathbf{r}_i}{}' \{1 - \exp[-tw(\mathbf{r}_i - \mathbf{r}_0)]\}\right), \qquad (4)$$

which is, in fact, the exact decay of Eq. (2) under the Poisson law $g(j) = e^{-p}p^j/j!$.

The decay laws, Eqs. (3) and (4), depend explicitly on the position $\mathbf{r}_0$ of the donor. In some physical situations the position of the donor is random, and hence, in order to obtain the experimentally accessible decay one has to average over $\mathbf{r}_0$.[21–23] As an example, for a finite volume and with $\mathbf{r}_0$ homogeneously distributed[22] ($N+1$ sites and L acceptors):

[a)] On leave from Max-Planck-Institut für Polymerforschung, Mainz and Lehrstuhl fur Theoretische Chemie, Technische Universitat München, West Germany.

$$\hat{\Phi}(t) = \frac{1}{N+1} \sum_{\mathbf{r}_0 \in V} \left[\frac{1}{N} \sum_{\mathbf{r} \neq \mathbf{r}_0} f(t, \mathbf{r}, \mathbf{r}_0) \right]^L . \quad (5)$$

We now concentrate on a given donor position $\mathbf{r}_0$ and focus on Eq. (4), which resembles most the original Förster forms.[1,9] By introducing a site-density function $\rho(\mathbf{r})$ we can transform the sum in Eq. (4) to the usual integral form. We set

$$\rho_0(\mathbf{r}) \equiv \sum_{\mathbf{r}_i}{}' \delta(\mathbf{r} - \mathbf{r}_i) , \quad (6)$$

where the index 0 in $\rho_0(\mathbf{r})$ acts as a reminder that $\mathbf{r}_0$ is excluded from the sum of the right-hand side. With $\rho_0(\mathbf{r})$ one obtains

$$\tilde{\Phi}(t,\mathbf{r}_0) = \exp\left(-p \int d\mathbf{r}\, \rho_0(\mathbf{r}) \{1 - \exp[-tw(\mathbf{r} - \mathbf{r}_0)]\} \right). \quad (7)$$

From Eq. (7) one now arrives at the Förster-type decays by taking $\rho_0 = (\mathbf{r}) = \rho =$ const and extending the integration over the whole space. We will in the following use different forms for $\rho_0(\mathbf{r})$ to model several restricted geometries and to display crossover effects.

III. EXAMPLES OF DECAY LAWS IN RESTRICTED GEOMETRIES

In this section we will display excluded volume effects, and the role of confined geometries on particular decay forms. These aspects are obtained by choosing appropriately the form of $\rho_0(\mathbf{r})$. We consider isotropic multipolar interactions:

$$w(\mathbf{r}) = \alpha r^{-s} \quad (s \geqslant 6) . \quad (8)$$

From Eq. (7) the following integral has to be evaluated:

$$I(t,\mathbf{r}_0) \equiv \int d\mathbf{r}\, \rho_0(\mathbf{r}) \{1 - \exp[-\mathrm{t}w(\mathbf{r} - \mathbf{r}_0)]\} . \quad (9)$$

We start with an infinite volume and consider the influence of a minimal distance b of approach between donor and acceptors.[7] Thus,

$$\rho_0(\mathbf{r}) = \begin{cases} 0 & \text{for } |\mathbf{r} - \mathbf{r}_0| < b \\ \rho & \text{otherwise} \end{cases} , \quad (10)$$

and one has for Eq. (9):

$$I(t, \mathbf{r}_0) = 4\pi\rho \int_b^\infty dr\, r^2 [1 - \exp(-t\alpha r^{-s})] \equiv I(t) , \quad (11)$$

which, because of the infinite volume, does not depend on $\mathbf{r}_0$ anymore. Setting $x = t\alpha\, r^{-s}$, $b_0 = t\alpha b^{-s}$, Eq. (11) reverts to

$$\begin{aligned} I(t) &= (4\pi\rho/s)(t\alpha)^{3/s} \int_0^{b_0} dx\, x^{-(s+3)/s} (1 - e^{-x}) \\ &= (4\pi\rho/3)(t\alpha)^{3/s} \\ &\quad \times \left[\int_0^{b_0} dx\, x^{-3/s} e^{-x} - b_0^{-3/s} (1 - e^{-b_0}) \right] \end{aligned} \quad (12)$$

which can be expressed in terms of the incomplete gamma function.[24]

We now consider the limiting cases of short and long times. At longer times $t \gg R^s/\alpha$ one has $b_0 \gg 1$ and Eq. (12) leads to

$$I(t) = (4\pi\rho/3)(t\alpha)^{3/s} \Gamma(1 - 3/s) , \quad (13)$$

i.e., the typical Förster-like decay,[1] where $\Gamma(z)$ is the Euler-gamma function[24]

$$\tilde{\Phi}(t, \mathbf{r}_0) \equiv \tilde{\Phi}(t) = \exp[-(4\pi/3)p\rho\Gamma(1 - 3/s)(t\alpha)^{3/s}] . \quad (14)$$

At shorter times $t \ll R^s/\alpha$, $b_0 \ll 1$, Eq. (12) gives

$$I(t) \approx 4\pi\rho\, b_0^{1-3/s} (t\alpha)^{3/s}/(s-3) = 4\pi\rho b^{3-s} t\alpha/(s-3) , \quad (15)$$

a linear dependence on t. The decay law follows thus an exponential behavior at short times:

$$\tilde{\Phi}(t) = \exp[-4\pi(s-3)^{-1} p\rho b^{3-s} \alpha t] \quad (16)$$

which is observable[7] in the exact decay, Eq. (3).

As the next example, we consider the acceptors to be distributed in a sphere of radius R, and calculate the decay for several donor positions. Taking first the donor at the center of the sphere $\mathbf{r}_0 = \mathbf{0}$, one has

$$\rho_0(\mathbf{r}) = \begin{Bmatrix} \rho & \text{for } r < R \\ 0 & \text{otherwise} \end{Bmatrix} . \quad (17)$$

Inserting Eqs. (17) and (8) into Eq. (7) one obtains

$$I(t, \mathbf{0}) = 4\pi\rho \int_0^R dr\, r^2 [1 - \exp(-t\alpha r^{-s})] . \quad (18)$$

As in the previous example, with $x_0 = t\alpha R^{-s}$, it follows

$$\begin{aligned} I(t, \mathbf{0}) = (4\pi\rho/3)(t\alpha)^{3/s} \Big[&\Gamma(1 - 3/s) + x_0^{-3/s} (1 - e^{-x_0}) \\ &- \int_0^{x_0} dx\, x^{-3/s} e^{-x} \Big] . \end{aligned} \quad (19)$$

For $R \to \infty$ one has $x_0 \to 0$ and only the Förster term, Eq. (14) remains on the right-hand side of Eq. (19). The second and third term on the right-hand side are the finite volume corrections, which depend, via x_0, on the radius R. These correction terms become important at longer times. For R fixed and large t, $t \gg R^s/\alpha$ one has $x_0 \gg 1$ and Eq. (19) turns into

$$I(t, \mathbf{0}) \sim (4\pi\rho/3)(t\alpha)^{3/s} x_0^{-3/s} = (4\pi/3)\rho R^3 . \quad (20)$$

The decay according to Eq. (7) is for large t,

$$\tilde{\Phi}(t, \mathbf{0}) \approx \exp[-p\rho(4\pi R^3/3)] \quad (21)$$

and is hence a nonzero, time-independent value. Equation (21) states that the probability that the donor does not decay at all is simply that of not finding any acceptor inside the volume $4\pi R^3/3$.

Let us consider the short-time behavior of Eq. (19). For fixed R and small t, $t \ll R^s/\alpha$, one has $x_0 \ll 1$, and we again obtain the Förster-type behavior, Eq. (14). Thus for finite R the decay law $\tilde{\Phi}(t, \mathbf{0})$ shows a crossover behavior at intermediate times $t \approx R^s/\alpha$ from the Förster-type form to a constant, nonzero value.

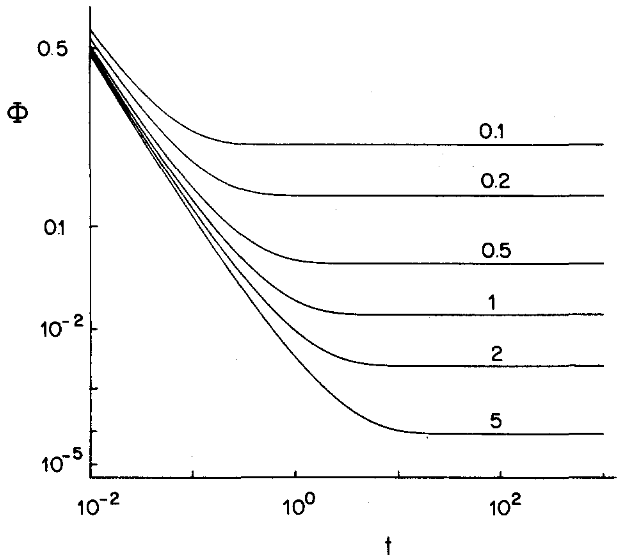

FIG. 1. Decay law Φ of an excited donor centered in a sphere with randomly distributed acceptors. The interactions are dipolar $w(r) = ar^{-6}$, and the decays are parametrized according to the value of $w(R)$ on the sphere, which goes from 0.1 to 1.0. Note the $-\ln[\ln \Phi]$ vs $\ln t$ scales.

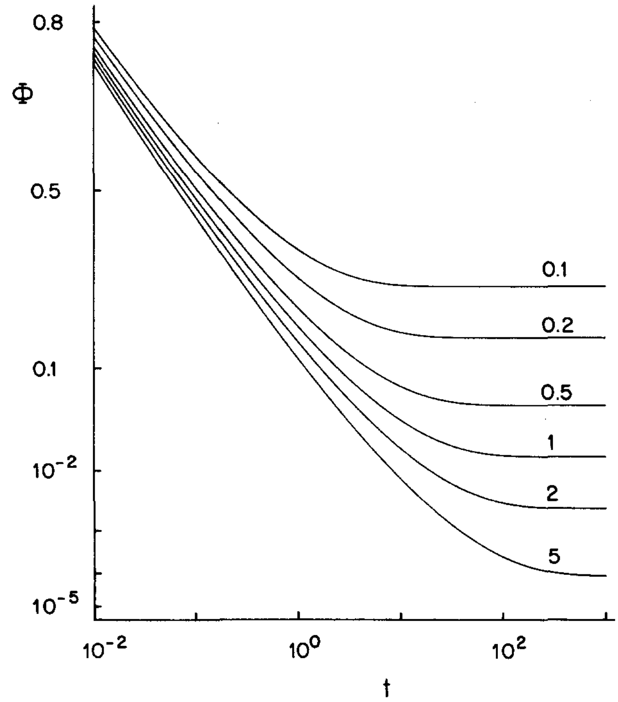

FIG. 2. Same as Fig. 1, with the donor placed on the surface of the sphere.

In order to display the crossovers, and to facilitate the comparison with experimental findings which result from such restricted geometries, we present in Fig. 1 the decay laws for several values α, such that $w(\mathbf{R})$ varies between 0.1 to 10. The decays are plotted as $-\ln[-\ln \Phi]$ vs $\ln t$. In these scales the short- and long-time forms appear as two different straight lines, with a crossover region between them, as is evident from Fig. 1. All decays scale with ρ, and we have thus set $\rho = 1$.

To display the dependence of $\tilde{\Phi}(t, \mathbf{r}_0)$ on $\mathbf{r}_0$ we now consider the donor to be placed on the surface of the sphere, say on the z axis, at $\mathbf{R}_0 = (0, 0, R)$. Using spherical coordinates centered at $\mathbf{R}_0$, one obtains

$$\rho_0(r)dr = \rho r^2\, dr \int_0^{2\pi} d\psi \int_0^{\theta_{\max}} \sin\theta\, d\theta$$
$$= 2\pi r^2(1 - r/2R)\rho\, dr \qquad (22)$$

with $\theta_{\max} = \arccos(r/2R)$. Inserting Eq. (22) into Eq. (9) we obtain

$$I(t, \mathbf{R}_0) = 2\pi\rho \int_0^{2R} dr\, r^2[1 - \exp(-tar^{-s})]$$
$$-(\pi\rho/R)\int_0^{2R} dr\, r^3[1 - \exp(-tar^{-s})]\,. \qquad (23)$$

Letting R go to infinity, we retrieve, apart from a factor of 2 the Förster form, Eqs. (13) and (14), namely,

$$\tilde{\Phi}(t, \mathbf{R}_0) = \exp[-(2\pi/3)p\rho\Gamma(1 - 3/s)(t\alpha)^{3/S}]\,. \qquad (24)$$

The difference by a factor of 2 in the exponents of Eqs. (14) and (24) is due to the fact that now the donor sees only one-half of the space occupied by acceptors.

We now consider the corrections due to the finite volume. At long times $t \gg (2R)^s/\alpha$, the $\exp(-tar^{-s})$ terms in Eq. (23) may be neglected and

$$I(t, \mathbf{R}_0) = 2\pi\rho(2R)^3/3 - (\pi\rho/R)(2R)^4/4 = (4\pi/3)\rho R^3\,, \qquad (25)$$

i.e., again a constant. The short-time behavior of Eq. (23) may be found along lines similar to those leading to Eq. (14). We obtain for small times,

$$I(t, \mathbf{R}_0) = (2\pi\rho/3)(t\alpha)^{3/s}\Gamma(1 - 3/s)$$
$$-(\rho/4R)(t\alpha)^{4/s}\Gamma(1 - 4/s) + \cdots, \qquad (26)$$

i.e., the Förster decay for the half-space, Eq. (24), corrected so as to obtain a slower decay at moderate times $t \lesssim (2R)^s/\alpha$. The direction of the correction is evident, since the half-space seen by the donor is not completely accessible to the acceptors.

These decays are presented in Fig. 2; and they differ from Fig. 1 only through the placement of the donor on the surface of the sphere. As seen by comparing Eqs. (18) and (23), or Figs. 1 and 2, for restricted geometries $I(t, \mathbf{r}_0)$ depends in general on the position $\mathbf{r}_0$ of the donor. As stated before, Eq. (5), if the donors occupy randomly the volume V, one has to average over their possible positions in order to obtain the experimental decay form:

$$\Phi(t) = \int d\mathbf{r}_0 \rho(\mathbf{r}_0)\Phi(t, \mathbf{r}_0)$$
$$\approx \int d\mathbf{r}_0 \rho(\mathbf{r}_0)\exp[-pI(t, \mathbf{r}_0)]\,. \qquad (27)$$

When the $I(t, \mathbf{r}_0)$ are basically similar, one may well approximate the decay law through the averaged exponent (first cumulant):

$$\Phi(t) \approx \exp\left[-p\int d\mathbf{r}_0 \rho(\mathbf{r}_0) I(t, \mathbf{r}_0)\right]. \qquad (28)$$

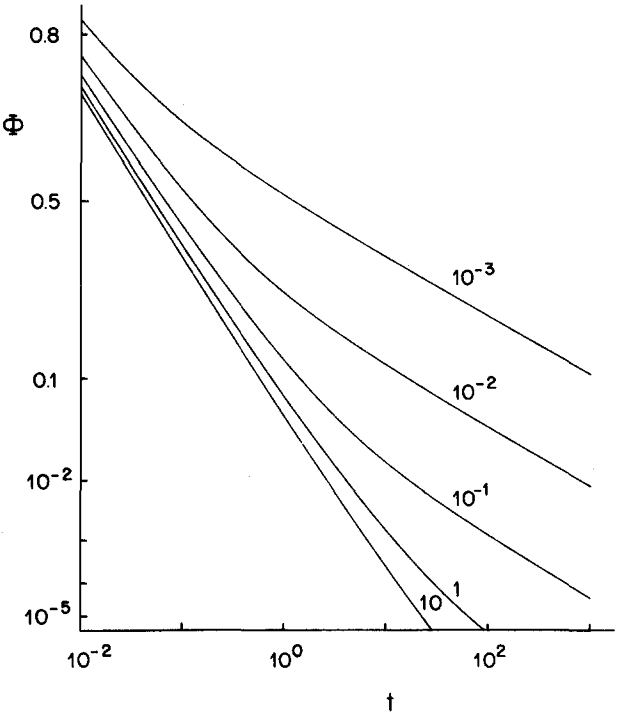

FIG. 3. Decay law Φ of an excited donor placed on the surface of a cylinder of radius R. The symbols are as in Fig. 1.

Examples for which Eq. (28) holds are for instance angular-dependent dipolar interactions,[25] whose decay laws display large deviations in the corresponding $I(t)$ forms and which (apart from a numerical factor of about 0.85), are well described by such cumulant averages.

As a third type of decay which can be obtained by considerations on $\rho_0(\mathbf{r})$ we now treat the direct transfer to acceptors distributed in a cylinder of radius R. Let the donor be located on the surface of the cylinder at the origin $\mathbf{0} = (0, 0, 0)$. The axis of the cylinder lies at a distance R from the origin and points along the z direction, and thus

$$\rho_0(r)dr\,dz = 2r\rho \arccos(r/2R)\mathrm{d}r\,\mathrm{d}z\,. \tag{29}$$

Inserting Eq. (29) into Eq. (9) we obtain

$$I(t, \mathbf{0}) = 4\int_0^{2R} dr \int_0^{\infty} dz\, r\rho \arccos(r/2R) \times\{1 - \exp[-t\alpha(r^2 + z^2)^{-s/2}]\}\,. \tag{30}$$

In the cylindrical case, as in the spherical volume example, for short times $t \ll R^2/\alpha$ one recovers the Föster-type decay, Eq. (24), where the donor sees only half the space occupied by acceptors. For the long-time decay, $t \gg R^2/\alpha$, Eq. (30) yields the Förster decay corresponding to one dimension

$$\tilde{\Phi}(t, \mathbf{0}) = \exp[-p\rho 2\pi R^2 \Gamma(1 - 1/s)(t\alpha)^{1/s}]\,. \tag{31}$$

Thus, the cylindrical geometry leads to a crossover between a three-dimensional and a one-dimensional Förster-type behavior. Here again the geometrical restriction induces a slower relaxation of the donor. The corresponding decays are given in Fig. 3.

To show again the influence of the position of the donor, we give in Fig. 4 the decays corresponding to a donor on the axis of the cylinder. Here

$$\rho_0(\mathbf{r})dr\,dz = 2\pi r\rho\,dr\,dz \tag{32}$$

and thus

$$I(t, R) = 4\pi \int_0^{R} dr \int_0^{R} dz\, r\rho \times\{1 - \exp[-t\alpha(r^2 + z^2)^{-s/2}]\}\,. \tag{33}$$

The long-time behavior of Eq. (33) is again given by Eq. (31).

Summarizing, in this paper we have displayed deviations from Förster-type behavior for the direct energy transfer on restricted geometries. The decay laws show crossovers and a richer pattern than that which obtains for regular infinite lattices. In all the cases studied the smooth site density function $\rho_0(\mathbf{r})$ accounts well for the geometrical restrictions which enter the direct energy transfer decay laws. While for the finite spherical volume the long-time decay crosses over to constant value (zero dimension), in the case of cylinders the crossover is from three-to-one dimension, Eq. (31). Further types of crossovers are readily envisaged.

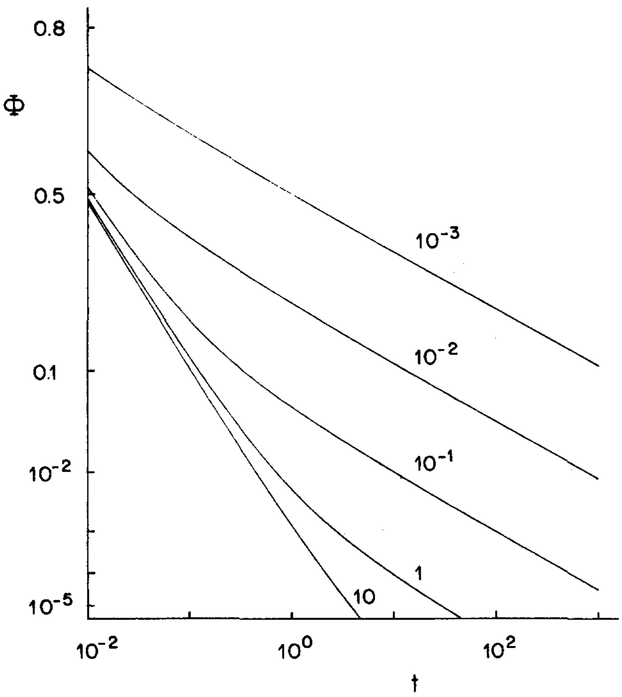

FIG. 4. Same as Fig. 3, with the donor placed on the cylinder axis.

ACKNOWLEDGMENTS

Our thanks are due to Professor J. Jortner for helpful discussions. The hospitality of the Exxon Corporate Research Science Laboratories and research grants from the Fonds der Chemischen Industrie and the Deutsche Forschungsgemeinschaft are gratefully acknowledged by A. B. The computations were rendered possible by a grant of computer time from the ETH-Rechenzentrum.

[1]T. Förster, Z. Naturforsch. Teil A **4**, 321 (1949).
[2]D. L. Dexter, J. Chem. Phys. **21**, 836 (1953).
[3]M. Inokuti and F. Hirayama, J. Chem. Phys. **43**, 1978 (1965).
[4]R. Katraro, A. Ron, and S. Speiser, Chem. Phys. Lett. **52**, 16 (1977).
[5]S. Speiser, Appl. Phys. **19**, 165 (1979).
[6]D. L. Huber, in *Laser Spectroscopy of Solids*, edited by W. M. Yen and P. M. Selzer (Springer, New York, 1981), p. 85.
[7]A. Blumen and J. Manz, J. Chem. Phys. **71**, 4694 (1979).
[8]A. Blumen, J. Chem. Phys. **72**, 2632 (1980).
[9]A. Blumen, Nuovo Cimento B **63**, 50 (1981).
[10]A. Blumen, J. Chem. Phys. **74**, 6926 (1981).
[11]J. Klafter and A. Blumen, in *Energy Transfer Processes in Condensed Matter*, edited by B. DiBartolo (Plenum, New York, 1984).
[12]D. Rehm and K. B. Eisenthal, Chem. Phys. Lett. **9**, 387 (1971).
[13]G. Porter and C. J. Tredwell, Chem. Phys. Lett. **56**, 278 (1978).
[14]U. K. A. Klein and H. P. Haar, Chem. Phys. Lett. **58**, 531 (1978).
[15]Y. Kusumoto and H. Sato, Chem. Phys. Lett. **68**, 13 (1979).
[16]R. Sh. Mikhail and E. Robens, *Microstructure and Thermal Analysis of Solid Surfaces* (Wiley, New York, 1983).
[17]M. D. Ediger and M. D. Fayer, Macromolecules **16**, 1839 (1983).
[18]R. Reisfeld, N. Manor, and D. Avnir, Solar Energy Mater. **8**, 399 (1983).
[19]U. Even, K. Rademann, J. Jortner, N. Manor, and R. Reisfeld, Phys. Rev. Lett. **52**, 2164 (1984).
[20]B. B. Mandelbrot, *The Fractal Geometry of Nature* (Freeman, San Francisco, 1982).
[21]C. L. Yang, P. Evesque, and M. A. El-Sayed, J. Phys. Chem. (to be published).
[22]J. Klafter and A. Blumen, J. Chem. Phys. **80**, 875 (1984); J. Lumin. **34**, 77 (1985).
[23]M. D. Ediger and M. D. Fayer, J. Chem. Phys. **78**, 2518 (1983).
[24]M. Abramowitz and A. Stegun, *Handbook of Mathematical Functions* (Dover, New York, 1972).
[25]H. Kellerer and A. Blumen, Biophys. J. **46**, 1 (1984).
[26]A. Blumen, J. Klafter, and G. Zumofen, Phys. Rev. B **28**, 6112 (1983).
[27]J. Klafter, A. Blumen, and G. Zumofen, J. Stat. Phys. **36**, 553 (1984).